

1 **Environmental assessment of a new generation battery:**
2 **The magnesium-sulfur system**

3
4 Claudia Tomasini Montenegro^a, Jens F. Peters^b, Manuel Baumann^c,
5 Zhirong Zhao-Karger^a, Christopher Wolter^d and Marcel Weil^{*a,c}

6
7 ^aHelmholtz Institute Ulm for Electrochemical Energy Storage (HIU), Ulm, Germany.

8 ^bUniversity of Alcalá (UAH), Faculty of Economics, Alcalá de Henares, Madrid, Spain

9 ^cInstitute for Technology Assessment and System Analysis (ITAS), Karlsruhe Institute of Technology (KIT), Karlsruhe, Germany.

10 ^dCustom Cells Itzehoe GmbH, Fraunhoferstraße 1b, Itzehoe, Germany.

11
12 *Corresponding contributor. E-mail: marcel.weil@kit.edu

13 **Abstract**

14 As environmental concerns mostly drive the electrification of our economy and the corresponding
15 increase in demand for battery storage systems, information about the potential environmental impacts
16 of the different battery systems is required. However, this kind of information is scarce for emerging
17 post-lithium systems such as the magnesium-sulfur (MgS) battery. Therefore, we use life cycle
18 assessment following a cradle-to-gate perspective to quantify the cumulative energy demand and
19 potential environmental impacts per Wh of the storage capacity of a hypothetical MgS battery (46
20 Wh/kg). Furthermore, we also estimate global warming potential (0.33 kg CO₂ eq/Wh) , fossil
21 depletion potential (0.09 kg oil eq / Wh), ozone depletion potential (2.5E-08 kg CFC-11/Wh) and metal
22 depletion potential (0.044 kg Fe eq/Wh), associated with the MgS battery production. The battery is
23 modelled based on an existing prototype MgS pouch cell and hypothetically optimised according to the
24 current state of the art in lithium-ion batteries (LIB), exploring future improvement potentials. It turns
25 out that the initial (non-optimised) prototype cell cannot compete with current LIB in terms of energy
26 density or environmental performance, mainly due to the high share of non-active components,
27 decreasing its performance substantially. Therefore, if the assumed evolutions of the MgS cell
28 composition are achieved to overcome current design hurdles and reach a comparable lifespan,
29 efficiency, cost and safety levels to that of existing LIB; then the MgS battery has significant potential
30 to outperform both existing LIB, and lithium-sulfur batteries.

31
32 **Keywords:** life cycle assessment, energy storage, post-lithium battery, lithium-ion battery and climate
33 change

35 Introduction

36 The energy sector is and will remain a cornerstone of the social and economic development of society.
37 Thus, the transition towards limiting the global temperature between 1.5 and a maximum of 2.0 degrees
38 Celsius threshold, as defined in the Paris Agreement [1, 2], depends on the identification of pathways
39 that contribute to the decarbonisation process of this sector, which account for 29% of the direct carbon
40 emissions [1]. Consequently, the integration of renewable energy sources and the development of
41 energy storage systems that enhance the flexibility of the power systems, while allowing them to buffer
42 fluctuations associated with variable renewable energy, is a crucial factor to reach the energy-related
43 sustainable development goals (i.e. SDG3: ensure healthy lives and promotes well being for all at ages,
44 SDG7: affordable and clean energy and SDG13: take urgent action to combat climate change and its
45 impacts) [3, 4]. Despite the dominance of pumped hydro storage systems, batteries, and more
46 specifically lithium-ion batteries (LIB), have become a crucial technology for this kind of service
47 (contributing to 41% of the 0.34 GW non-pumped hydro storage) [5]. Also, there is a soaring demand
48 for LIB for the transport sector, which faces similar challenges in terms of decarbonisation [6, 7].

49 The recent success of LIB in these sectors is explained by their excellent performance, namely their
50 high energy density, high power rate capability, long life cycle and flexible scaling [6]. Nevertheless,
51 especially for the transport sector, further improvements are required for them to become mass
52 technology. The main challenges for current LIB in this regard are: (i) improved energy density (300
53 Wh/kg), (ii) cost reductions (below 100 US/kWh) [4], (iii) increased lifetime (10 years) [8], (iv)
54 reduction of the content of scarce and critical resources [9, 10], and (v) reduced risk of dendrite
55 formation [11, 12]. In particular, questions about the environmental impacts, demand for critical and
56 scarce resources, and recyclability have come to the centre of public debate recently [4]. These
57 concerns are becoming more and more relevant during the decision-making process about different
58 energy storage options [13, 14]. It is recognised that to avoid environmental burden shifting, the
59 estimation of these impacts should be conducted considering a holistic approach along the life cycle of
60 the LIB [14, 15]. Currently, such evaluation is carried out using life cycle assessment (LCA), which is
61 an environmental assessment tool that considers inputs and outputs to estimate the potential
62 environmental impacts associated with a product system [16, 17]. In the European Union, a harmonised
63 version of the life cycle approach has served as a basis of the Single Market Green Initiative, a unified
64 set of rules that promotes understanding of the trade-offs, on an environmental basis, of commercially
65 available products, which includes LIB rechargeable batteries [18].

66 To overcome the environmental constraints of current LIB, research on other battery chemistries is
67 conducted to identify new technologies with competitive performance, but reduced environmental
68 impacts and material requirements [5, 12]. Regarding the latter, the elimination of cobalt and nickel,
69 but also copper and lithium, are within the scope, all associated with different concerns about their
70 future availability and high environmental impacts during the mining phase [9]. Among the prospective
71 potential candidates, magnesium-sulfur (MgS) batteries are considered as one of the most promising
72 options to manage these concerns regarding safety, energy density, environmental impacts and resource

73 availability associated with LIB [19, 20]. Concerning energy density, the advantage of the MgS cell is
74 explained by the divalent Mg^{+2} nature, theoretically offering almost double the volumetric capacity
75 compared to lithium [19, 21]. Furthermore, MgS cells are also safer due to the potential absence of
76 dendrite formation for magnesium [21]. They are expected to have significant potential for cost
77 reduction, relying on widely available and cheap materials like metallic magnesium for the anode
78 manufacture [22, 23]. Thus, when combined with a sulfur cathode, the MgS electrochemical couple is a
79 promising, high capacity, low cost and safe post-lithium option [23-25].

80 While the environmental impacts of LIB have been assessed by numerous works and with different
81 scopes (see the comprehensive reviews presented by Sullivan *et al.* [26, 27] and Peters *et al.* [28]), this
82 information is scarce for post-LIB options, with only a handful of assessments of sodium ion, lithium-
83 sulfur, lithium-air, composite cathode, and advanced LIB published recently [28-33]. For MgS, the
84 only existing environmental assessment is based on a laboratory pouch cell in a configuration [34].
85 Therefore, this work aims to fill this gap by conducting an LCA of a theoretical MgS battery according
86 to the ISO standards 14040/44 [16, 17], establishing the following objectives:

- 87 • (i) development of the life cycle inventory for the MgS cell and battery;
- 88 • (ii) identification of the main hot spots associated not just with global warming, but also other
89 environmental impacts that include fossil, metal and ozone depletion potential;
- 90 • (iii) quantification of the cumulative energy demand (CED) associated with the life cycle of the
91 MgS battery;
- 92 • (iv) provide a theoretical horizon of the environmental performance of the theoretical MgS
93 battery analysed in this work.

94 The results are compared with current lithium-based options, more specifically, a lithium-iron-
95 phosphate (LFP) [33, 35], and a lithium nickel-manganese-cobalt (NMC) battery [35, 36].
96 Furthermore, a lithium-sulfur (LiS) battery is also considered as a benchmark for a possible
97 evolutionary stage after current LIB [30]. This information will set the scene for the future
98 assessment of MgS batteries, which might be required to quantify the associated environmental
99 impacts and contribute to establishing guidelines for optimising upcoming MgS prototypes under
100 eco-design aspects [37].

101

102 Methods

103 Goal and scope definition

104 The goal of this study is twofold. Firstly, it is aimed at the identification and quantification of the
105 environmental impacts associated with a theoretical MgS battery based on the MgS cell developed by
106 Wagner *et al.* [38]. Secondly, the hot spots of the estimated environmental impacts will also be
107 identified. The scope of the LCA of the MgS battery is from cradle to gate, considering 1 Wh of energy
108 storage capacity provided by the battery on a battery pack level as the functional unit (the unit of
109 reference for estimating and comparing potential environmental impacts). The following impact
110 categories are calculated based on the mid-point hierarchic perspective of the ReCiPe 2008 impact
111 assessment method [39], using Open LCA version 1.9 [40]: (i) global warming potential (GWP), i.e.,
112 climate change, is the most present environmental concern in society currently; (ii) ozone depletion
113 potential (ODP), i.e., the impact on the decomposition of the ozone layer ('ozone hole'), (iii) metal
114 depletion potential (MDP), i.e., the depletion of abiotic mineral resources, being the use of scarce
115 metals of particular concern for lithium batteries and one of the arguments used for promoting
116 alternative battery chemistries [9], and (iv) fossil depletion potential (FDP), since, despite current
117 efforts to shift toward cleaner energy resources, fossil energy still contributes 40% to the European
118 electricity mix [41]. Additionally, the cumulative energy demand (CED) is calculated as an indicator of
119 the total energy investment (renewable and non-renewable) required for the manufacture of the battery,
120 including all upstream processes and inputs [42, 43]. It is considered as a useful summary ('footprint')
121 indicator during the decision-making process related to the sustainability assessment of batteries, but
122 also energy technology in general [44-46]. Finally, the impact of the electricity supply, which has been
123 identified as a hot spot, is revised in a sensitivity analysis.

124

125 Data sources and assumptions

126 The life cycle inventory (LCI) of the MgS battery system under analysis is developed based on a hybrid
127 approach. As a result, primary data obtained for an existing prototype pouch cell is used to model both
128 cell components and assembly of the MgS cell [38, 47]. Since the inventory data has been derived
129 primarily from a prototype pouch cell, a hypothetical industrial-scale production needs to be assumed
130 for a meaningful assessment and comparison with existing secondary batteries. Here, we rely on data
131 available for current lithium battery options, being the main comparable process steps of cell
132 manufacture [31]. Both data sources and assumptions corresponding to each element of the inventory
133 are given below. Information for the background system has been sourced from the ecoinvent database
134 version 3.5 [48]. A detailed description of individual LCI is provided in the supplementary information.

135

137 The pilot-scale MgS cell layout described in Table 1 forms the basis of our battery model. The cell is
138 composed of an Mg foil anode combined with a sulfur cathode and an $\text{Mg}[\text{B}(\text{hfp}_4)_2] \cdot \text{DME}$
139 (magnesium tetrakis hexafluoroisopropoxy borate with dimethoxyethane as organic solvent)
140 electrolyte, hereafter referred to as $\text{Mg}[\text{B}(\text{hfp}_4)_2]_2$ (0.3M) [38]. The magnesium foil serves both as
141 anode and anode current collector. At the same time, the sulfur is coated onto an aluminium foil current
142 collector with a 5% black carbon additive for increased conductivity, and 5% carboxy-methyl-
143 cellulose/styrene-butadiene rubber (CMC/SBR) polymer binder. Cathode and anode are separated by a
144 polyolefin membrane, which makes up 10% of the total cell mass in the prototype. The whole-cell is
145 assembled in a simple (and comparably thick) pouch housing. Due to the preliminary stage of the
146 development of this cell, information about its performance in terms of cycle life and efficiency is not
147 available. Still, information about the energy density of this early version prototype cell is available,
148 amounting to 57 Wh/kg on pouch cell level.

149 For this reason, we rely on a theoretical battery model and optimise the layout of the MgS cell
150 assuming a hypothetical future commercial cell, allowing the evaluation of its potential environmental
151 impacts in comparison with different battery types. However, due to the specific challenges associated
152 with the electrochemistry of the MgS system [21, 49, 50], we only modify the passive components.
153 Consequently, the cell is optimised regarding the share of the pouch cell housing and separator, using
154 average values achieved by current LIB as targets. These components are selected because based on
155 their high contribution to the mass share in the prototype battery cell, they are assumed to be subject to
156 optimisation once produced commercially. In particular, the following (hypothetical) targets are set: (i)
157 reduced cell pouch mass share from 45% wt. (baseline battery configuration; MgS-BL) to 3% wt.
158 (MgS-Evo1),

159 Moreover, (ii) reduce the thickness and correspondingly the mass share of the separator from 10% wt.
160 to 2% wt. (MgS-Evo2), corresponding to the current state of the art in LIB [51]. The composition of
161 each version of the MgS cell is given in Table 1. Information about the procedure to estimate the
162 composition of each configuration is given in the supplementary material.

163 Due to the early stage in the research and development of the MgS battery, no information about its
164 potential commercial applications is available. Thus, it is assumed that the MgS cells are mounted in an
165 automotive battery pack with a configuration similar to that of current LIB packs, considering an
166 average composition of 5.5% BMS, 14.5% casing and 80% cell [51]. Also, due to the absence of
167 further information in this regard, the battery pack composition has been assumed equal for each MgS
168 cell layout (MgS-BL MgS-Evo1 and MgS-Evo2). The mass share of cells is maintained constant for the
169 different evolutions, assuming that increasing energy density of the cells leads to an improved storage
170 capacity of the battery pack while maintaining the same size and weight. Information about the
171 estimated energy density on a cell and battery level is provided in Table 1. The procedure to calculate
172 the composition of the optimised MgS cell Evo1 and Evo2 is detailed in the supplementary information.

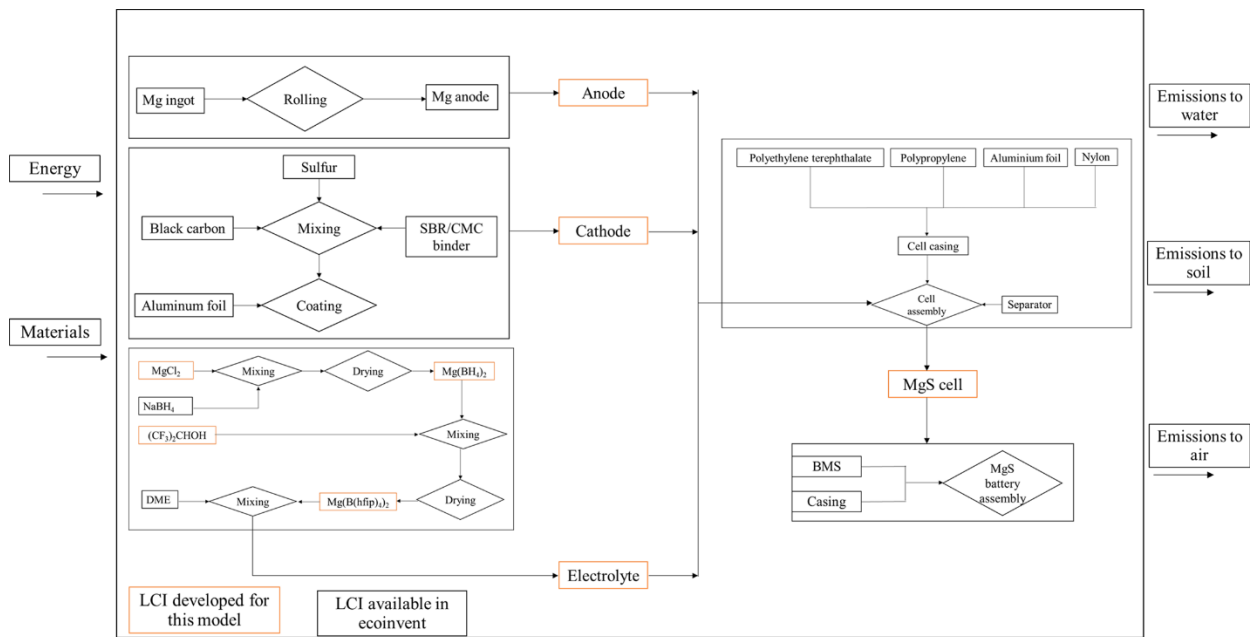
173 **Table 1** Composition of the original and optimised MgS cell. MgS-BL: Baseline MgS cell (prototype cell as provided by
 174 Wagner et al. [38]). MgS-Evo1: First optimisation with reduced cell package mass; MgS-Evo2: Second optimisation with
 175 reduced separator thickness

Item	Material	MgS-BL (mg)	(%wt.)	MgS- Evo1 (mg)	(%wt.)	MgS- Evo2 (mg)	(%wt.)
Battery cells							
Anode	Mg foil	427	6.4	427	11.2	427	29.0
Cathode	Sulfur	421	6.3	421	11.1	421	28.7
	Binder	5	0.1	5	0.13	5	0.3
	Carbon	5	0.1	5	0.13	5	0.3
	Al Collector foil	88	1.3	88	2.3	88	6
Separator	Polyolefin	700	10.4	700	18.3	29	2
Electrolyte	Mg[B(hfip) ₄] ₂ •DME	2060	30.7	2060	53.9	451	30.7
Housing	Al composite	3000	44.7	115	3	44	3
Total (cell)		6706	100	3821	100	1478	100
Energy density (cell)	--	57 Wh/kg	--	100 Wh/kg	--	259 Wh/kg	--
Battery pack (1 kg)							
Battery cells		0.8 kg	80%	0.8 kg	80%	0.8 kg	80%
Pack housing		0.145 kg	14.5%	0.145 kg	14.5%	0.145 kg	14.5%
BMS		0.055 kg	5.5%	0.055 kg	5.5%	0.055 kg	5.5%
Total (pack)		0.20 kg	20%	0.20 kg	20%	0.20 kg	20%
Energy density (pack)		46Wh/kg	--	80Wh/kg	--	207Wh/kg	--

176

177 System and system boundaries

178 As shown in Figure 1, the system boundaries of the MgS product system under analysis includes the
 179 manufacturing of the cell components and battery assembly.



180

181

Figure 1 System boundary of the MgS battery product system

182 Both use and recycling phases are disregarded due to insufficient knowledge about achievable cycle
 183 life and long-term stability. Before evaluating the MgS battery on an application level, the challenges
 184 associated with avoiding the formation of passivating layers need to be overcome [52]. Regarding the
 185 recycling phase, as pointed out by Mohr *et al.*, available information about the environmental impacts
 186 of the recycling of lithium-ion batteries is scarce, and mainly based on unspecific data about the
 187 recycling process or the composition of the waste stream [53]. This stage should be carefully modelled
 188 to quantify the environmental impacts of the reuse of LIB [29, 54]. Therefore, due to the prevailing
 189 lack of data about the recycling of battery chemistries already consolidated in the market, information
 190 about future candidates such as the MgS battery is either null or not freely available. For this reason,
 191 this life cycle stage has not been considered within the system boundary of this analysis. This limits the
 192 study up to a certain point, but eliminates additional uncertainties from assumptions for these life cycle
 193 stages, and allows the estimation of targets in terms of cycle life that the MgS battery needs to achieve
 194 for competing with existing LIB.

195 Life cycle inventory

196 MgS cell inventory

197 As seen in Figure 1, the LCI of the elements of the manufacture of the MgS cell encompasses data for
 198 the anode, cathode, electrolyte, cell housing and separator. Electricity supply required for both battery
 199 and cell manufacture has been modelled based on the European electricity mix. Due to the lack of
 200 information about anode manufacture, it is assumed that the production process of Mg foil is similar to
 201 that of other metal foils, like aluminium. For the rolling process, aluminium sheet rolling is considered
 202 as a valid proxy, as the rolling processes of Al and Mg show similar energy demands and associated

203 CO₂ emissions [55]. In both cases, Mg ingot manufacture and the rolling process are sourced from
204ecoinvent 3.5 [48]. According to Wolter *et al.* [56], the thickness of 100µm for the anode foil is
205determined primarily by practical aspects, i.e., the commercial availability of foil with this thickness.
206Information for the background system has been sourced from the ecoinvent database version 3.5 [48].
207A detailed description of individual LCI is provided in the supplementary information.

208For proprietary reasons, the exact manufacturing process of the cathode is not disclosed, but its
209composition can be derived from the data available for the reference pilot MgS cell [38]. This process
210consists of a mixture of sulfur, black carbon and (CMC/SBR) polymer binder in mass ratios of (5:4:1).
211The cathode manufacturing process is modelled assuming a slurry-casting process similar to that of
212LIB, where the slurry mixture is cast on the aluminium current collector [57]. While background
213inventory data for electricity, heat and infrastructure, sulfur and black carbon have been sourced from
214ecoinvent 3.5 [48], the LCI of the CMR/SBR binder stems from Peters *et al.* [31]. Because of its
215electrochemical characteristics, in combination with its stability in the ambient atmosphere (air and
216water), Mg[B(hfip)₄]₂ (0.3M), is used as the electrolyte for the MgS cell [25]. The synthesis of the
217electrolyte salt Mg[B(hfip)₄]₂ is based on the dehydrogenation reaction of Mg(BH₄)₂ with (CF₃)₂CHOH
218(hfip)[47], with the corresponding inventory data for hfip and its precursors estimated based on the
219hydrogenation of hexafluoroacetone [58].

220Since no industrial-scale manufacturing process of Mg [B(hfip)₄]₂ is yet developed, both energy and
221infrastructure requirements have been approximated based on industrial sodium tetrafluoroborate
222production [59]. As explained above, the manufacturing process of post-lithium batteries such as the
223MgS battery is assumed as similar to those of LIB; therefore, electricity and heat requirements for the
224cell and battery pack assembly processes are derived from averaged aggregated data from LCA studies
225on LIB production [51]. The components of the battery pack (housing, auxiliary components and
226battery management system) are modelled according to the current state of the art for LIB [36, 51].

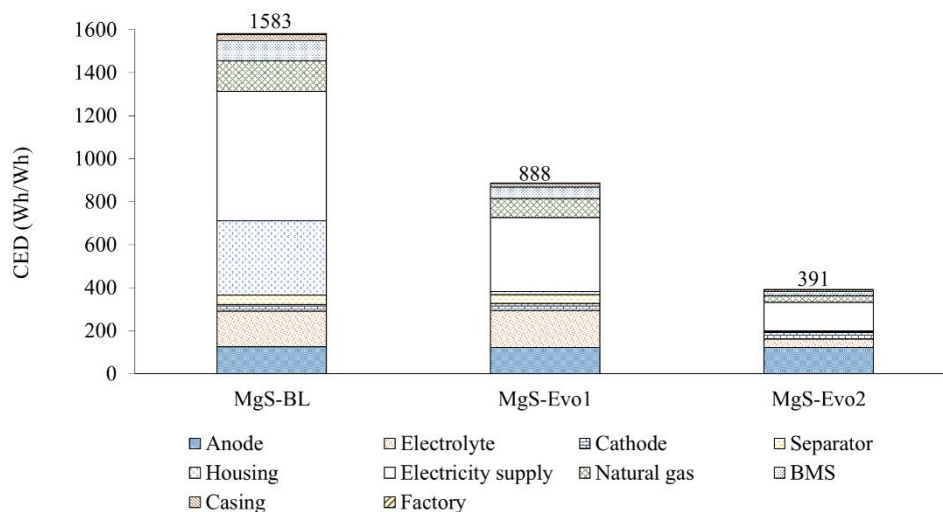
227 Results

228 Cumulative energy demand (CED)

229Figure 2 provides the CED results for the three MgS cell configurations. For the baseline cell
230configuration (MgS-BL), the high contribution of the cell housing is evident, driven mainly by the
231aluminium content of the pouch and its energy-intensive production. Reducing the mass of the pouch
232housing (MgS-Evo1) not only reduces the contribution of the pouch housing, but also increases the
233energy density of the cell (less inactive material in the cell), and therefore reduces the impact of all
234other non-active components proportionally. The second optimisation (MgS-Evo2) reduces the
235thickness of the separator, also affecting the amount of electrolyte, and thus further reducing total
236energy demand.

237As seen in Figure 2, the CED associated with this cell amounts to 1583 Wh. This value can be
238considered as the total energy investment (including all upstream energy inputs along the process chain)

239 and needs to be amortised during battery use. In this sense, it also gives a certain lower limit for the
 240 lifetime of the battery, since with lifetimes < 390 cycles the energy investment will always be higher
 241 than the return.



242
 243 **Figure 2** CED associated with the three MgS battery configurations. Legend (MgS-BL: baseline layout according to
 244 prototype cell; MgS-Evo1: first evolution with optimised pouch housing; MgS-Evo2: second evolution with optimised
 245 separator thickness and the correspondingly lower amount of electrolyte)

246 Environmental profile of the MgS-battery

247 A summary of the environmental profile of the MgS battery configurations is given in Figure 3. Overall,
 248 the higher the energy density, the lower the environmental impacts. Similar to the CED results, the two
 249 evolutions of the baseline cell configuration (MgS-Evo1 and MgS-Evo2) show significantly lower
 250 environmental impacts than the baseline MgS-BL. A detailed analysis of the contribution of each
 251 component for the three different MgS battery configurations is given for each impact category in the
 252 following section.

253 Global warming potential

254 The contribution of the anode represents 41% and 20% of the total estimated GWP associated with
 255 MgS-Evo2 and MgS-Evo1, respectively. The majority of these greenhouse gas emissions can be
 256 explained by the electricity requirements of the Mg foil manufacture from the Pidgeon process (91%),
 257 which is the main route to magnesium production [60]. The electricity requirements for the assembly of
 258 the cell and battery manufacture respectively make up another 25% and 32% of the total GWP of the
 259 MgS-Evo2 and MgS-Evo1 batteries. The electrolyte is identified as the third hot spot, respectively
 260 contributing 17% and 7% for the GWP associated with MgS-Evo1 and MgS-Evo2. This contribution is
 261 explained by the electricity requirements for the manufacture of the salt ($Mg[B(hfip)_4]_2$) (39%) (see
 262 Figure 3).

263 Fossil depletion

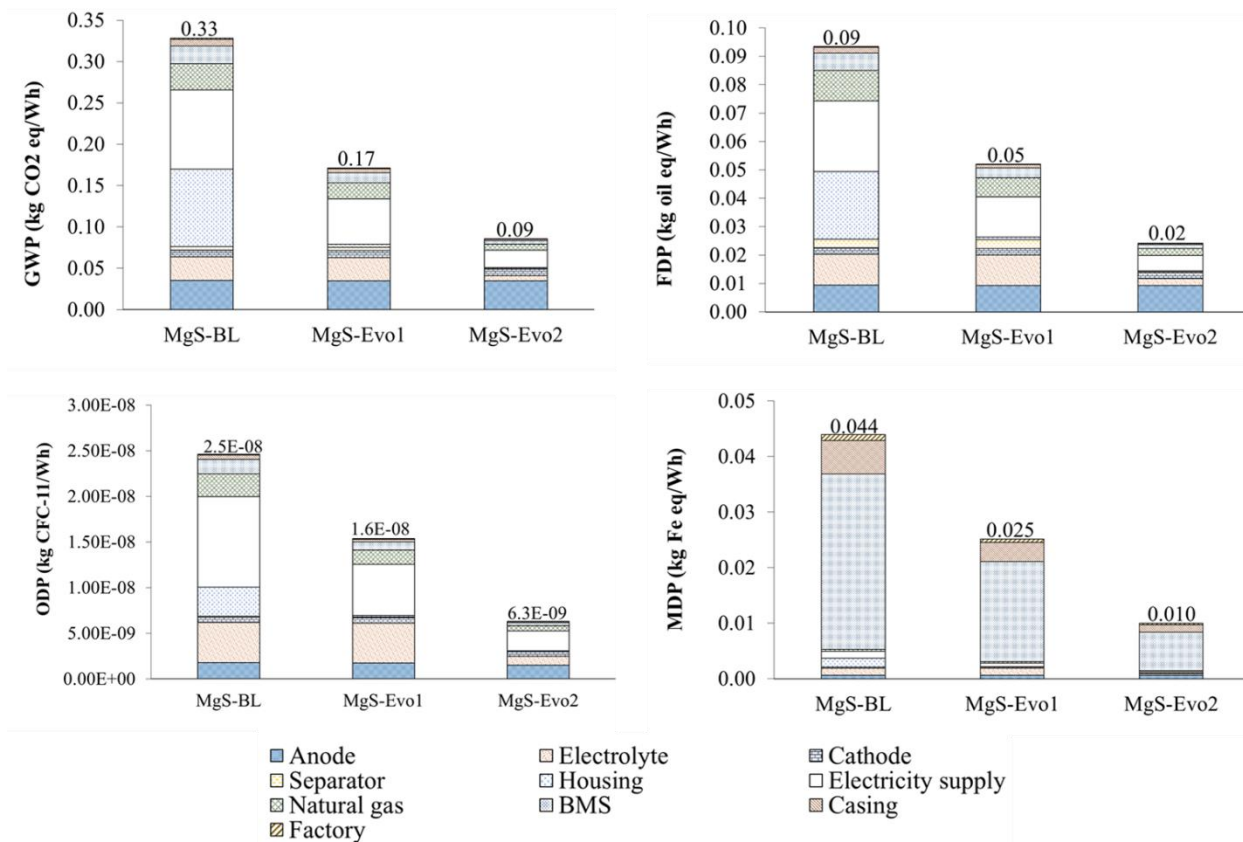
264 As seen in Figure 3, anode manufacture can be identified as the central hot spot (39% of the total FDP),
265 followed by the electricity required for the manufacturing process (mainly cell assembly) (27%) and
266 electrolyte manufacture (10%). The main contribution of the FDP associated with the MgS-Evo1
267 battery comes from electricity supplied for cell and battery manufacture (27%). Additionally, the shares
268 of the electrolyte (21%) and anode manufacture (18%) are identified as the second and third hot spots
269 for this battery pack. About 61% of the electrolyte's share is caused by the manufacture of the salt
270 ($\text{Mg}[\text{B}(\text{hfiip})_4]_2$, due to its electricity requirements (30%). The depletion of fossil resources associated
271 with anode manufacture is mainly created by the magnesium foil manufacturing process (99%).

272 Metal depletion potential

273 The contribution of the BMS represents the main hot spot (71%) of the estimated MDP associated with
274 the MgS-Evo1 and MgS-Evo2, which is followed by the contribution from the casing of the battery
275 pack (14%). Although information about the BMS and the casing of the MgS batteries is still missing,
276 these results indicate that on a battery pack level, the components are critical drivers of the estimated
277 MDP. As expected, the MgS battery cell itself hardly shows any MDP impacts, as it contains no scarce
278 or critical materials.

279 Ozone depletion potential

280 Electricity supply for battery and cell manufacturing dominate the ODP of the MgS batteries, followed
281 by the electrolyte for MgS-BL (18%) and MgS-Evo1 (29%), as well as the anode for MgS-Evo2 (24%);
282 and thermal energy required for the manufacturing process. These decrease with increasing energy
283 density and therefore, with the subsequent optimisation stages.



284 **Figure 3** Contribution analysis of the selected ReCiPe environmental impacts of the MgS-BL, MgS-Evo1 MgS-
 285 Evo2 batteries. Legend (MgS-BL: baseline layout according to prototype cell; MgS-Evo1: first evolution with
 286 optimised pouch housing; MgS-Evo2: second evolution with optimised separator thickness and the
 287 correspondingly lower amount of electrolyte.

288 Comparison between the environmental impacts of the MgS battery and lithium batteries

289 To situate the results for the MgS battery within the current landscape, environmental impacts of the
 290 MgS battery are compared with three current technologies. These have been selected based on the
 291 maturity of the lithium battery market for automotive applications: 1) a nickel-manganese-cobalt
 292 lithium battery NMC, based on Ellingsen *et al.* (NMC (EII)) and Majeau-Bettez *et al.* (NMC (M-B))
 293 [35, 36]; 2) lithium-iron-phosphate (LFP), based on Zackrisson *et al.* (LFP (Zak)) and Majeau-Bettez *et al.*
 294 (LFP (M-B)) [33, 35], and 3) a theoretical lithium-sulfur (LiS (Deng)) battery considered to be a
 295 potential candidate as a future substitute for the LIB [30], based on a hybrid approach considering
 296 laboratory and pilot-scale information for the cell manufacture [30]. For these three systems, the
 297 specific layout and corresponding environmental impacts are estimated based on data from previous
 298 studies [30, 33, 35, 36], with the energy densities normalised by assuming identical cell housings and
 299 battery pack layout [51] (See Table 2).

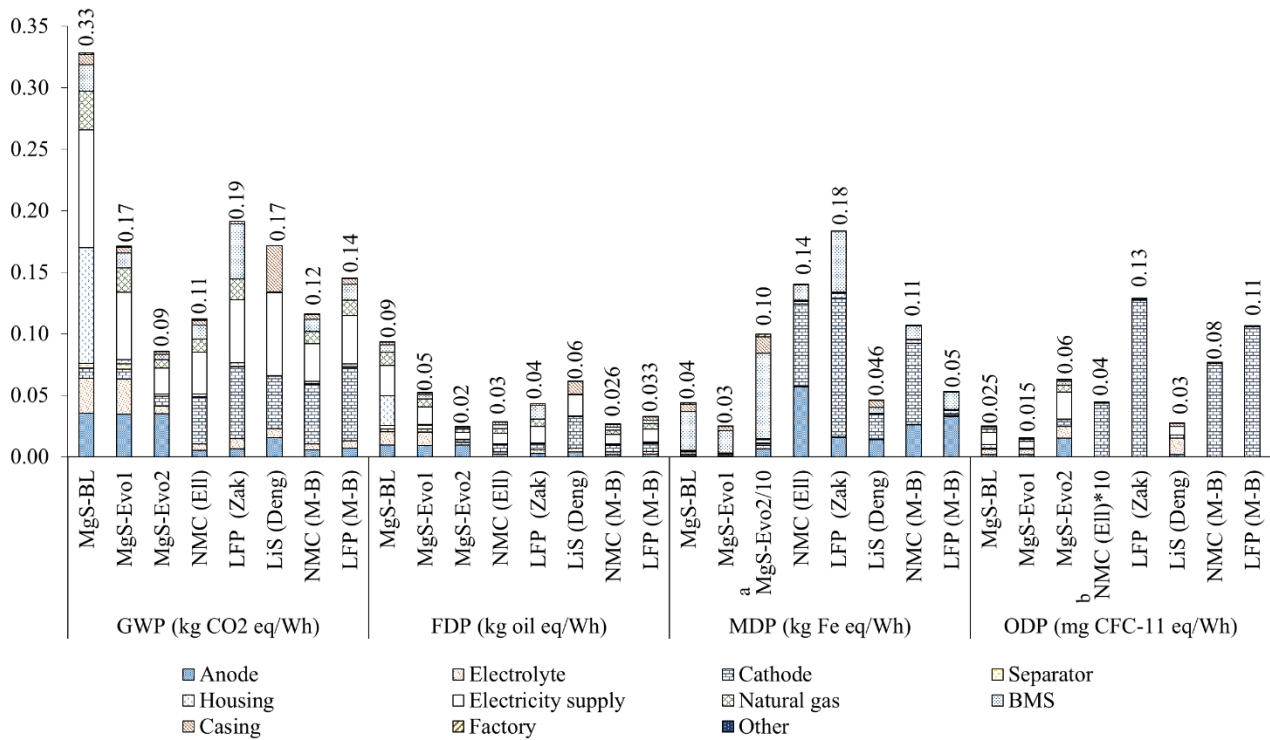
300

Table 2 Energy density, NMC and LiS battery systems

Battery chemistry	Energy density Wh/kg (original value)	Energy density Wh/kg (adjusted value)
NMC (Ell) [36]	105.1	130.3
LFP (Zak) [33]	93	86.4
LiS (Deng) [30]	220	224
NMC (M-B) [35]	112	144.85
LFP (M-B) [35]	88	113.8

302 The **GWP** results are displayed in Figure 4. The baseline MgS-BL shows by far the highest impacts,
303 but reducing the mass of the pouch housing (MgS-Evo1) reduces the GWP impact to that of the LiS
304 battery. However, further, improvement is needed to outperform the LIB. Due to a reduction in the
305 amount of electrolyte being soaked up by the separator, this improvement is achieved by reducing the
306 thickness of the separator to values similar to that of current LIB, as modelled in the MgS-Evo2.
307 The CO₂eq. emissions from the cathode represent the leading cause to the total GWP associated with
308 the LFP (Zak), LFP (M-B) and NMC (M-B), contributing to 30.5% to the former and 41% to both LFP
309 (M-B) and NMC (M-B). These contributions are explained by the emissions associated with
310 tetrafluoroethylene manufacture. As seen in Figure 4, the electricity supply for the cell and battery
311 assembly is the central hot spot for the other battery types, with a contribution between 25% for MgS-
312 Evo2 up to 39% for the LiS. Still, the contribution to GWP of the remaining components is very
313 different. For the MgS-Evo2 the second hot spot is the anode (40%), but for the LiS and the LIB, it is
314 the cathode, contributing 25% and 36% to the total GWP, respectively.

315 Except for the LiS, **FDP** is dominated by the electricity demand for battery manufacture, 26% MgS-BL;
316 31% NMC (Ell); 30% (M-B)), followed by the cathode for the lithium-based batteries 20% (NMC (Ell);
317 21% NMC (M-B); 20% LFP (M-B); 43% LiS (Deng)), and the BMS for the LFP (Zak) (26%). The
318 share of the electrolyte is also representative for magnesium-based batteries (21% MgS-Evo1; 10%
319 MgS-Evo2), while for the baseline cell configuration MgS-BL, the cell pouch contributes the
320 significant share with 26% of the total FDP.



321

322 **Figure 4** Comparison between the environmental impacts associated with the MgS and lithium batteries

323 Legend (MgS-BL: baseline layout according to prototype cell; MgS-Evo1: first evolution with optimised pouch
 324 housing; MgS-Evo2: second evolution with optimised separator thickness and the correspondingly lower amount
 325 of electrolyte. (NMC (EII)) nickel-manganese-cobalt lithium battery based on Ellingsen *et al.* [36]; (LFP (Zak))
 326 lithium-iron-phosphate (LFP), based on Zackrisson *et al.*[33]; (LiS (Deng)) lithium-sulfur based on Deng *et al.*
 327 [30]; (NMC (M-B)) and (LFP (M-B)) nickel-manganese-cobalt lithium battery and lithium-iron-phosphate based
 328 on Majeau-Bettez *et al.* [35]. a: This value must be divided by 10 to obtain the original value. b: This value must
 329 be multiplied by 10 to obtain the original value

330 The **ODP** of the MgS batteries is mainly caused by the electricity demand for battery manufacture
 331 (MgS-BL: 40%; MgS-Evo1: 36%; MgS-Evo2: 34%), followed by the electrolyte (MgS-BL: 17.7%;
 332 MgS-Evo1: 28%; MgS-Evo2: 15.3%). For the NMC (EII) 91%, NMC (M-B) 99%, and LFP (Zak) 98%,
 333 LFP (M-B) 99%, the main contribution is attributed to cathode manufacture. Tetrafluoroethylene
 334 emissions explain these contributions to air from the binder manufacture (99%). While for the LiS
 335 (Deng), the electrolyte (47%) is the main hot spot for ODP, followed by the electricity supply (25%).

336 Under **MDP** aspects the BMS is the dominant contributor for all MgS batteries (72% MgS-BL; 71%
 337 MgS-Evo1; 69% MgS-Evo2). Here, it becomes evident that the MgS batteries are exclusively made of
 338 abundant materials, which minimises the MDP impact to the extent that it becomes hardly visible in
 339 comparison to the battery pack periphery, such as pack housing and BMS. In contrast, except for the
 340 LFP (M-B) with the anode as the main contributor to MDP (62%), the lithium batteries show
 341 significantly higher MDP impacts. They are driven mainly by the cathode (53% NMC (EII); 62% NMC

342 (M-B); 47% LFP (Zak); 44% LiS (Deng)), and the anode materials (24%, 26% and 31%, 40% of the
343 total for NMC (M-B), NMC (Ell), LiS (Deng), and LFP (Zak), respectively). For the anode, the main
344 reason for this is the copper current collectors. In contrast, for the cathode, the main reason is the use of
345 cobalt and nickel in the cathode active material (NMC) and the aluminium current collector (LiS).

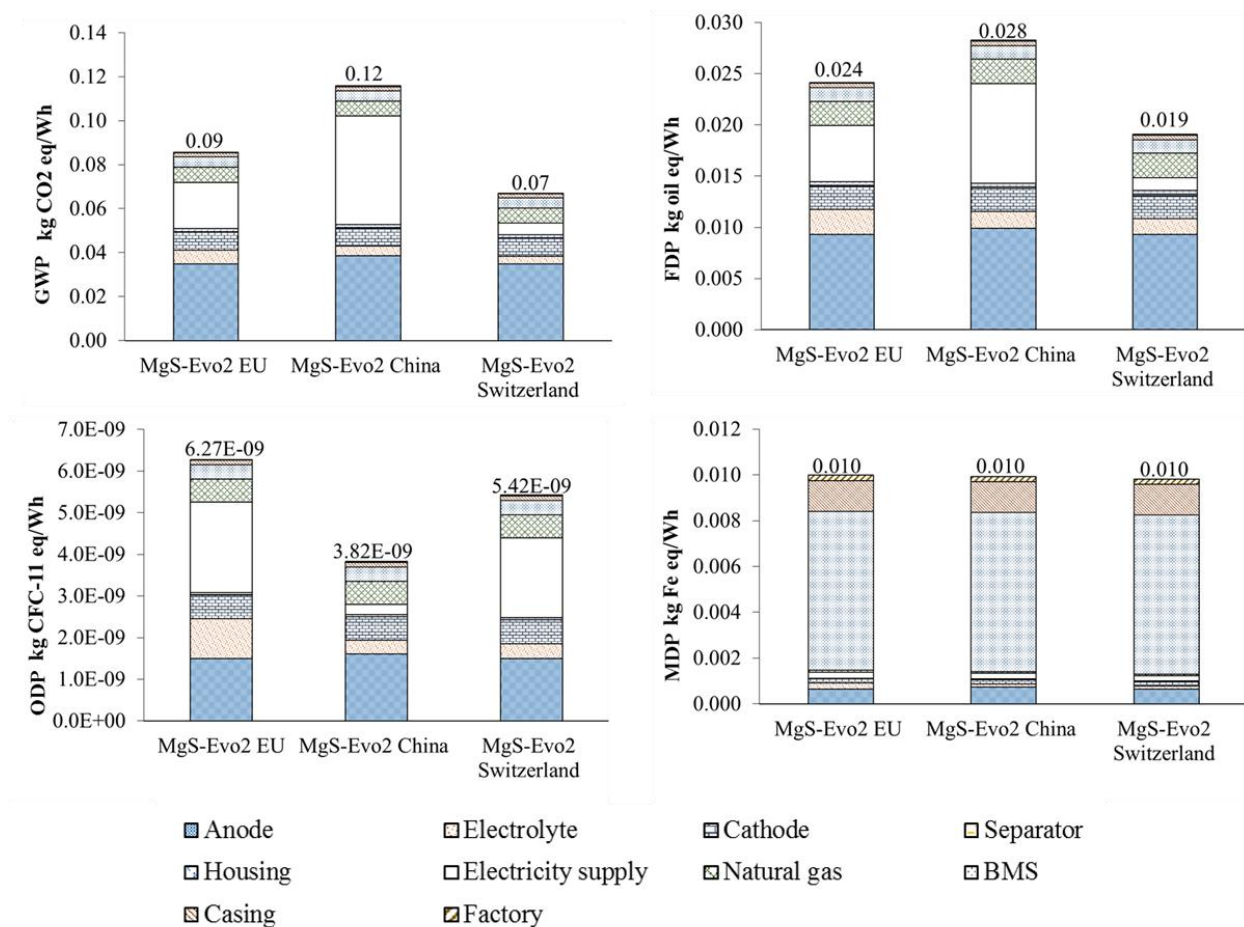
346 Sensitivity analysis

347 Electricity mix

348 The following sensitivity analysis assesses the influence of the electricity mix within our battery model.
349 As the MgS-Evo2 exhibits the best environmental performance, only this cell configuration is
350 considered.

351 The electricity supply for cell and battery pack manufacture is the central hot spot identified for the
352 environmental impacts of the MgS-Evo2. Thus, the use of the Chinese and Swiss electricity mixes, the
353 representative for an electricity mix of high (CN) and low carbon intensity (CH), is considered (for the
354 base case, the average EU electricity mix was assumed), with the corresponding results given in Figure
355 5. The composition of the EU and Swiss electricity mixes respectively include 30% and 33% of nuclear
356 power, in contrast with 2% in the Chinese electricity mix³⁵. As previously mentioned, due to the lack of
357 information about possible commercial manufacturing lines for MgS batteries, we initially assumed
358 that MgS and LIB manufacturing processes would have comparable energy demands. This assumption
359 might turn out to be inaccurate since one of the critical drivers for manufacturing energy demand is the
360 dry room required for handling the highly hygroscopic electrolyte of LIB. The MgS electrolyte used for
361 the prototype cell (Mg [B(hfip)₄]₂) (0.3M) is much less hygroscopic, and an optimised production line
362 might show significantly lower energy demand. However, in terms of environmental impacts, until
363 information about the actual manufacturing process of MgS batteries on a commercial level becomes
364 available, this might have similar consequences in the four assessed impact categories as changing to a
365 low-carbon electricity mix.

366



367

368 **Figure 5** Effect of the electricity mix on the environmental impacts associated with MgS-Evo2. Legend:
 369 MgS-Evo2 EU, MgS-Evo2 China, MgS-Evo2 Switzerland, MgS-Evo2: second evolution with
 370 optimised separator thickness and the correspondingly lower amount of electrolyte, respectively
 371 considering the European, Chinese and Swiss electricity mix.

372 Magnesium anode foil thickness

373 Since the anode foil is one of the drivers of environmental impacts in several of the assessed categories,
 374 we optimise the Mg foil thickness (in the prototype pouch cell determined by the simple availability of
 375 Mg foil with the given thickness on the market) according to electrochemical considerations. For this
 376 purpose, we calculate the area of the Mg foil based on the information available for the pouch cell and
 377 the mass of aluminium required to match the electrochemical potential of the sulfur cathode. Being the
 378 Mg foil both active material and current collector, a minimum thickness needs to be also maintained in
 379 a fully discharged state to assure current collection and avoid increasing ohmic losses. The minimum
 380 foil thickness for this purpose is estimated based on the conductivity of aluminium and magnesium,
 381 using the aluminium cathode thickness as a reference, and increasing the Mg foil thickness proportional
 382 to its higher specific ohmic resistance. Being the conductivity of magnesium roughly half that of
 383 aluminium, and the thickness of the cathode collector foil 4.4µm (88mg for an area of 74 cm² in the

384 prototype pouch cell), the resulting minimum magnesium foil thickness in the discharged state is 8.8
385 μm , equivalent to 113 mg Mg per pouch cell. The additional amount of magnesium required to match
386 the specific capacity of sulfur (1.67Ah/g) can be estimated based on electrochemical considerations.
387 With a specific capacity of sulfur of 2.21 Ah/g and a sulfur cathode load of 421mg/cell (see Table 1),
388 the required amount of magnesium anode active material amounts to 319 mg/cell. Adding the estimated
389 minimum foil thickness for assuring current collection functions even in a fully discharged state (113
390 mg), we obtain an optimised Mg foil mass of 432 mg, already slightly above that of the pouch cell
391 prototype. We can, therefore, state that, even if not directly intended but rather driven by pragmatic
392 reasons, the magnesium foil thickness is already at the lower limit and does not hold any further
393 optimisation potential.

394 Discussion

395 The results show that once the configuration of the MgS cell is optimised regarding the pouch cell
396 housing and the separator (MgS-Evo2), the composition of the electricity mix defines the pathway to
397 reduce its environmental impacts further. As discussed above, apart from the cell manufacturing
398 process itself, attention should also be given to the anode manufacturing process, which contributes the
399 second significant share and quickly becomes dominant when the impact from electricity for cell
400 manufacture decreases. Interestingly, the electricity supply in the magnesium manufacturing process is
401 the critical source of GHG emissions, so even here the sourcing of magnesium obtained by using
402 'green' electricity would be the clue to the improvement of environmental performance. Efforts to
403 improve the carbon footprint of the MgS battery should, therefore, focus on reducing the environmental
404 impacts of magnesium production (magnesium metal production is highly energy-intensive, and the
405 corresponding energy mix will be essential for this purpose). The effect of the optimisations assumed
406 for the MgS cells is also evident, eliminating the key contributors to GWP, including the large and
407 heavy cell pouch of the prototype MgS-BL, and subsequently optimising the thickness of the separator
408 and thus the amount of electrolyte (MgS-Evo2).

409 While the results for FDP are similar to those of GWP, the ODP results show different behaviour. Here,
410 the Chinese (coal-based) electricity mix gives better results; this is explained by the emissions from
411 uranium and natural gas manufacture, which overall are dominant for the CFC-114 and Halon-1301
412 emissions to air. These emissions from Swiss and European electricity mixes contribute 35% and 29%,
413 and 30% and 26% respectively to the total estimated ODP. Regarding metal depletion, cell
414 manufacturing energy plays an insignificant role in this impact category. Conversely, the composition
415 of the electricity mix used for cell manufacture or variations in the amount of electricity is negligible
416 (see Figure 5).

417 When comparing the $\text{CED}_{\text{total}}$ of the MgS batteries with the corresponding average value reported for
418 LIB (1.81 MJ/Wh) [28], the MgS-Evo2 achieves a lower cumulative energy demand. The main
419 contributor to the total CED for this optimised cell configuration is electricity supply (34% of the total;
420 mainly the energy requirements associated with cell manufacture), indicating this as a critical

421 assumption in the present assessment. Apart from electricity, anode manufacture is the second
422 contributor to MgS-Evo2, and here again, the electricity mix (and its carbon intensity) used for
423 producing the magnesium metal is the key for further reducing environmental impacts. A reduction of
424 the content of magnesium metal within the battery cell (as possible further evolution or optimisation
425 step) is found to be not reasonable, being the magnesium foil thickness already at the lower limit for
426 maintaining both electrochemical and current collector functions. In contrast, for the MgS-Evo1 cell
427 configuration, the electrolyte plays a significant role, and in the case of MgS-BL, the cell pouch
428 contributes substantially.

429 In summary, the optimised MgS batteries obtain promising results for all four evaluated impact
430 categories. In this first evolution stage (where only a reduction of the cell pouch mass to values similar
431 to those of current LIB is assumed; MgS-Evo1), their environmental impacts are already similar to or
432 below the LiS battery. If the second evolution stage can be achieved, MgS batteries have the potential
433 to outperform also current LIB, regarding the production phase.

434 Conclusions

435 We assessed the environmental performance of an MgS battery in three different configurations; a
436 prototype cell based on actual data from a project, and two hypothetical evolutions of this, with a
437 theoretical optimisation of the cell layout according to the current state of the art in lithium-ion battery
438 technology. The first prototype cell shows a comparably poor environmental performance due to
439 massive mass of pouch housing, thick separator and high amount of electrolyte. However, the
440 optimised cell layouts show an auspicious performance, with GWP impacts comparable to or even
441 better than those of current NMC and LFP type (LIB), and low impacts in mineral (metal) resource
442 depletion. A remaining key contributor to the majority of the four assessed environmental impact
443 categories is electricity demand along the process chain, in particular cell manufacture, where a similar
444 energy intensity to current LIB is assumed. Moreover, since the electrolyte of the MgS battery is less
445 hygroscopic, potentially avoiding the need for a dry room, which is one of the key drivers of
446 manufacturing energy demand for LIB, further reduction in the associated environmental impacts of the
447 MgS cell can be expected. If the magnesium production process were to rely on renewable electricity,
448 this would further reduce its environmental impacts.

449 If the assumed improvements to the current MgS cell layout can be achieved, then the MgS battery has
450 a high potential for outperforming its competitors LIB and LiS under environmental aspects. However,
451 this will only be possible if parameters that can be equally important for the total environmental
452 performance can also be achieved, e.g. comparable technical performance in terms of efficiency and
453 lifetime. These are not yet foreseeable and so are not evaluated further here, but they remain highly
454 relevant for future research regarding the overall environmental impacts of MgS batteries.

455 In this climate change context, which urges us to take action, the future of the post lithium will be
456 delimited not just by their performance but also by their associated environmental impacts. Hence, the

457 importance of the results presented in this work, which contribute to the identification and
458 quantification of these impacts associated with an MgS battery.

459 **Acknowledgments**

460 This work contributes to the research performed at CELEST (Center for Electrochemical Energy
461 Storage Ulm-Karlsruhe) and was funded by the German Research Foundation (DFG) under Project ID
462 390874152 (POLiS Cluster of Excellence), and was financially supported by the Initiative and
463 Networking Fund of the Helmholtz Association within the Network of Excellence on post-Lithium
464 batteries (ExNet-003

465

466 **References**

467

- 468 1. IPCC, Climate Change 2014: Synthesis Report. Contribution of Working Groups I, II and III to
469 the Fifth Assessment Report of the Intergovernmental Panel on Climate Change. Geneva,
470 Switzerland
- 471 2. IPCC, Global warming of 1.5°C. An IPCC Special Report on the impacts of global warming of
472 1.5°C above pre-industrial levels and related global greenhouse gas emission pathways, in the
473 context of strengthening the global response to the threat of climate change, sustainable
474 development, and efforts to eradicate poverty. . 2018, Intergovernmental Panel on Climate
475 Change: World Meteorological Organization, Geneva, Switzerland. p. 32.
- 476 3. IEA, World Energy Model 2019: Paris.
- 477 4. Edström, K., Battery 2030: Inventing the sustainable batteries of the future, research needs and
478 future actions 2020, Uppsala University
- 479 5. IEA, Tracking Clean Energy Progress 2017 2017, International Energy Agency Paris
- 480 6. Kim, T.H., et al., The current move of lithium-ion batteries towards the next phase. Advanced
481 Energy Materials, 2012. 2(7): p. 860-872.
- 482 7. Tsiropoulos, I., D. Tarvydas, and N. Lebedeva, Li-ion Batteries for Mobility and Stationary
483 Storage Applications Scenarios for Costs and Market Growth. Publications Office of the
484 European Union: Luxembourg, 2018.
- 485 8. Moseley, P.T. and J. Garche, Electrochemical energy storage for renewable sources and grid
486 balancing. 2014: Newnes.
- 487 9. Weil, M., S. Ziemann, and J. Peters, The Issue of Metal Resources in Li-Ion Batteries for
488 Electric Vehicles, in Behaviour of Lithium-Ion Batteries in Electric Vehicles. Ed.: G. Pistoia.
489 2018, Springer International Publishing, Cham. p. 59-74.
- 490 10. Commission, E., Study on the review of the list of critical raw materials. European Commission:
491 Brussels, Belgium, 2017.

- 492 11. Tarascon, J.-M. and M. Armand, Issues and challenges facing rechargeable lithium batteries, in
493 Materials For Sustainable Energy: A Collection of Peer-Reviewed Research and Review
494 Articles from Nature Publishing Group. 2011, World Scientific. p. 171-179.
- 495 12. Choi, J.W. and D. Aurbach, Promise and reality of post-lithium-ion batteries with high energy
496 densities. Nature Reviews Materials, 2016. 1(4): p. 16013.
- 497 13. Dehghani-Sanij, A., et al.. Study of energy storage systems and environmental challenges of
498 batteries. Renewable and Sustainable Energy Reviews, 2019. 104: p. 192-208.
- 499 14. Edström, K., Battery 2030+ Roadmap. 2020.
- 500 15. Finkbeiner, M., et al., Towards Life Cycle Sustainability Assessment. Sustainability, 2010.
501 2(10): p. 3309-3322.
- 502 16. International, ISO Standard., 14040: Environmental management–life cycle assessment–
503 principles and framework, L.B.S. Institution, Editor. 2006.
- 504 17. International, ISO Standard., 14044: Environmental management–life cycle assessment–
505 Requirements and Guidelines, B.S. Institution, Editor. 2006: London
- 506 18. EU, PEFCR - Product Environmental Footprint Category Rules for High Specific Energy
507 Rechargeable Batteries for Mobile Applications. 2018, European Commission
- 508 19. Fichtner, M., Magnesium Batteries: Research and Applications. 2019: Royal Society of
509 Chemistry
- 510 20. Choi, J.W. and D. Aurbach, Promise and reality of post-lithium-ion batteries with high energy
511 densities. Nature Reviews Materials, 2016. 1(4).
- 512 21. Bonnick, P. and J. Muldoon, A Trip to Oz and a Peak Behind the Curtain of Magnesium
513 Batteries. Advanced Functional Materials, 2020: p. 1910510.
- 514 22. Yoo, H.D., et al., Mg rechargeable batteries: an on-going challenge. Energy & Environmental
515 Science, 2013. 6(8): p. 2265.
- 516 23. Zhao-Karger, Z., et al., A new class of non-corrosive, highly efficient electrolytes for
517 rechargeable magnesium batteries. Journal of Materials Chemistry A, 2017. 5(22): p. 10815-
518 10820.
- 519 24. Zhao-Karger, Z., et al., Performance Improvement of Magnesium Sulfur Batteries with
520 Modified Non-Nucleophilic Electrolytes. Advanced Energy Materials, 2015. 5(3): p. 1401155.
- 521 25. Zhao-Karger, Z., et al., Toward Highly Reversible Magnesium–Sulfur Batteries with Efficient
522 and Practical Mg[B(hfip)4]2 Electrolyte. ACS Energy Letters, 2018. 3(8): p. 2005-2013.
- 523 26. Sullivan, J.L. and L. Gaines, Status of life cycle inventories for batteries. Energy conversion
524 and Management, 2012. 58: p. 134-148.
- 525 27. Sullivan, J.L. and L. Gaines, A review of battery life-cycle analysis: state of knowledge and
526 critical needs 2010, Argonne National Laboratory: Illinois U.S. p. 45.
- 527 28. Peters, J.F., et al., The environmental impact of Li-Ion batteries and the role of key parameters –
528 A review. Renewable and Sustainable Energy Reviews, 2017. 67: p. 491-506.
- 529 29. Cusenza, M.A., et al., Energy and environmental assessment of a traction lithium-ion battery
530 pack for plug-in hybrid electric vehicles. Journal of cleaner production, 2019. 215: p. 634-649.
- 531 30. Deng, Y., et al., Life cycle assessment of lithium sulfur battery for electric vehicles. Journal of
532 Power Sources, 2017. 343: p. 284-295.

- 533 31. Peters, J., et al., Life cycle assessment of sodium-ion batteries. *Energy & Environmental*
534 *Science*, 2016. 9(5): p. 1744-1751.
- 535 32. Salgado Delgado, M.A., et al., Comparative Life Cycle Assessment of a Novel Al-Ion and a Li-
536 Ion Battery for Stationary Applications. *Materials*, 2019. 12(19): p. 3270.
- 537 33. Zackrisson, M., et al., Life cycle assessment of lithium-air battery cells. *Journal of Cleaner*
538 *Production*, 2016. 135: p. 299-311.
- 539 34. Montenegro, C.T., Peters, J.F., Zhao-Karger, Z., Wolter, C. and Weil, M. . In *Magnesium*
540 *Batteries Life Cycle Analysis of a Magnesium–Sulfur Battery*, in *Magnesium Batteries:*
541 *Research and Applications*, R.S.o. Chemistry, Editor. 2019, Fichtner, M., Ingram, B.J.,
542 Sheridan, E., Mohtadi, R., Battaglia, C., Zhao-Karger, Z., Canepa, P., Dominko, R., Hoeche, D.,
543 Weil, M. and Yoo, H.D. p. 309-330.
- 544 35. Majeau-Bettez, G., T.R. Hawkins, and A.H. Transman, Life cycle environmental assessment of
545 lithium-ion and nickel-metal hydride batteries for plug-in hybrid and battery electric vehicles.
546 *Environmental science & technology*, 2011. 45(10): p. 4548-4554.
- 547 36. Ellingsen, L.A.W., et al., Life cycle assessment of a lithium-ion battery vehicle pack. *Journal of*
548 *Industrial Ecology*, 2014. 18(1): p. 113-124.
- 549 37. Schöggel, J.-P., R.J. Baumgartner, and D. Hofer, Improving sustainability performance in early
550 phases of product design: A checklist for sustainable product development tested in the
551 automotive industry. *Journal of Cleaner Production*, 2017. 140: p. 1602-1617.
- 552 38. Wagner, N., et al. development of magnesium-sulfur batteries: from fundamental research to
553 application in 2nd International Symposium on Magnesium Batteries. 2018. Ulm, Germany:
554 Helmholtz Institute Ulm.
- 555 39. Goedkoop M.J., et al., ReCiPe 2008, A life cycle impact assessment method which comprises
556 harmonised category indicators at the midpoint and the endpoint level; First edition Report I:
557 Characterisation. 6 January 2009.
- 558 40. GreenDeltaOpenLCA.
- 559 41. Moreno Ruiz, E., Valsasina L., Brunner, F., Symeonidis A., FitzGerald D., Treyer, K.,
560 Bourgault G., Wernet G., Documentation of changes implemented in ecoinvent database v3. 5,
561 in Zurich: ecoinvent. 2018, ecoinvent
- 562 42. Frischknecht, R., et al., Cumulative energy demand in LCA: the energy harvested approach.
563 *The International Journal of Life Cycle Assessment*, 2015. 20(7): p. 957-969.
- 564 43. Hischier R., et al., Implementation of Life Cycle Impact Assessment Methods. Ecoinvent report
565 No. 3, v2.2. 2010, Swiss Centre for Life Cycle Inventories: Dübendorf.
- 566 44. Notter, D.A., et al., Contribution of Li-ion batteries to the environmental impact of electric
567 vehicles. 2010, ACS Publications.
- 568 45. Zimmermann, B., et al. A comparative analysis of the cumulative energy demand of stationary
569 grid-integrated battery systems. In *2013 International Conference on Clean Electrical Power*
570 *(ICCEP)*. 2013. IEEE.
- 571 46. McManus, M.C., Environmental consequences of the use of batteries in low carbon systems:
572 The impact of battery production. *Applied Energy*, 2012. 93: p. 288-295.

- 573 47. Zhao-Karger, Z., et al., A new class of non-corrosive, highly efficient electrolytes for
574 rechargeable magnesium batteries. *Journal of Materials Chemistry A*, 2017. 5(22): p. 10815-
575 10820.
- 576 48. Moreno Ruiz, E., et al., Documentation of changes implemented in ecoinvent database v3. 5.
577 Ecoinvent: Zürich, Switzerland, 2018.
- 578 49. Song, J., et al., Mapping the Challenges of Magnesium Battery. *J Phys Chem Lett*, 2016. 7(9): p.
579 1736-49.
- 580 50. Wang, P. and M.R. Buchmeiser, Rechargeable Magnesium–Sulfur Battery Technology: State of
581 the Art and Key Challenges. *Advanced Functional Materials*, 2019. 29(49): p. 1905248.
- 582 51. Peters, J.F. and M. Weil, Providing a common base for life cycle assessments of Li-Ion batteries.
583 *Journal of Cleaner Production*, 2018. 171: p. 704-713.
- 584 52. Zhao-Karger, Z. and M. Fichtner, Magnesium–sulfur battery: its beginning and recent progress.
585 *MRS Communications*, 2017. 7(4): p. 770-784.
- 586 53. Mohr, M., et al., Toward a cell-chemistry specific life cycle assessment of lithium-ion battery
587 recycling processes. *Journal of Industrial Ecology*, 2020.
- 588 54. Bobba, S., et al., Life Cycle Assessment of repurposed electric vehicle batteries: an adapted
589 method based on modelling energy flows. *Journal of Energy Storage*, 2018. 19: p. 213-225.
- 590 55. Hakamada, M., et al., Life cycle inventory study on magnesium alloy substitution in vehicles.
591 *Energy*, 2007. 32(8): p. 1352-1360.
- 592 56. Wolter, C., Personal communication C.T. Montenegro, Editor. 2018.
- 593 57. Hagen, M., et al., Lithium–Sulfur Cells: The Gap between the State-of-the-Art and the
594 Requirements for High Energy Battery Cells. *Advanced Energy Materials*, 2015. 5(16): p.
595 1401986.
- 596 58. Yuzuru Morino, K., et al., Method for producing hexafluoroisopropanol and fluoromethyl
597 hexafluoroisopropyl ether (sevoflurane) L. Central Glass Company, Editor. 2017, Central Glass
598 Company, Limited: United States
- 599 59. Sutter, J., Life cycle inventories of highly pure chemicals. . 2007, Swiss Center for Life Cycle
600 Inventories: Dübendorf.
- 601 60. Wulandari, W., et al., Magnesium: current and alternative production routes. *Engineering at the
602 Edge*; 26-29 September 2010, Hilton Adelaide, South Australia, 347.

